XVII IMEKO World Congress
Metrology in the 3rd Millennium
June 22−27, 2003, Dubrovnik, Croatia

HIGH PRECISION INSTRUMENT FOR MICRO SURFACE PROFILE MEASUREMENT BASED ON OPTICAL INVERSE SCATTERING PHASE METHOD

Atsushi TAGUCHI, Takashi MIYOSHI, Yasuhiro TAKAYA, and Satoru TAKAHASHI

Department of Mechanical Engineering and Systems, Osaka University, Osaka, Japan

Abstract − With the advance of microtechnology, in-process or *in situ* measurement techniques for measuring surface profiles of engineered micro parts have been increasingly required. We have proposed an optical measurement technique, the optical inverse scattering phase method, which can be applied to the in-process measurement of micro-surface profile with the accuracy in the nanometer order. An instrument has been designed and developed on the basis of the proposed principles, and verified by measuring an ultra precision grid plate having rectangular pockets 44nm deep at intervals of 10μm. The measured surface profile gave good agreement with the nominal dimensions of the specimen as well as the one obtained by AFM.

Keywords: Micro-surface profile, Fraunhofer diffraction, phase retrieval

1. INTRODUCTION

With the advance of micro technology, ever-improving metrology is required in the production of precision-engineered micro parts. In-process or *in situ* quality inspection of the dimensional characteristics of the engineered surface is an essential tool for ensuring a cost-effective production with high quality. We need a novel profiler that is at the same time fast, high precision, non-contact as well as non-destructive with a long working distance, robust against the vibrations in a production environment, simple operation without onerous technical setup, and able to be adapted to automation.

We have developed an optical profiler on the basis of the optical scattering phase method, which has been proposed in our recent work[1][2]. In the present method, spectral information of a surface profile is obtained by measuring Fraunhofer diffraction intensity. By employing phase retrieval technique[3–5], surface profile is reconstructed from the measured diffraction intensity deterministically (not statistically). Some advantages of the present method are the following: a surface profile within the whole illuminated area can be measured simultaneously, no scanning process is imposed; a long working distance is achievable with no contact to work surface; there is no requirement of precise positioning of the measured work; measurements of diffraction intensity are not likely to be affected by vibrations; and thus, the possibility of near-process or in-process implementation.

Here we describe the general principles of the proposed method, the optical instrumentation, and the experimental results carried out. The instrument consists basically of a modified optical microscope, which enables one to measure Fraunhofer diffraction intensity with high accuracy. The developed instrument was verified by measuring a surface topography reference that was designed for characterizing SPM. Measured surface profile gave good agreement with the nominal dimensions of the specimen as well as the one obtained by AFM.

2. OPTICAL INVERSE SCATTERING PHASE METHOD

2.1. Measurement principles

An object having surface profile $h(x,y)$ is located in the object plane Π, as shown in Fig. 1. The object surface is coherently illuminated by a plane monochromatic wave incident normally onto the plane Π. The complex amplitude

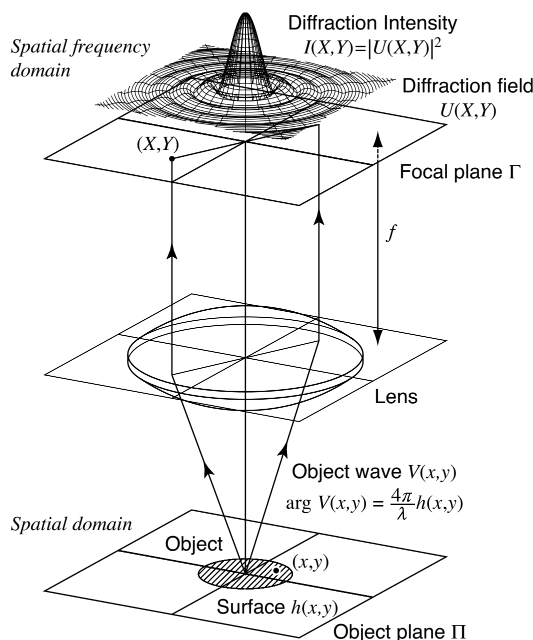

Fig. 1. Schematic illustration of the measurement principles.

of the scattering light from the surface (we will refer to this as object wave here) is expressed as

$$V(x,y)=|V(x,y)|\exp[i\theta(x,y)] \qquad (1)$$

The object wave is regarded as a result of interactions between the incident light and the illuminated object. Here, we assume $\theta(x,y)$, the phase part of the object wave, is a function of the surface profile $h(x,y)$ and the wavelength of the incident light λ, in accordance with

$$\theta(x,y)=\frac{4\pi}{\lambda}h(x,y) \qquad (2)$$

To determine the phase $\theta(x,y)$ is of our interest; when the phase is determined, we can calculate surface profile $h(x,y)$ by using (2) conversely.

The object wave $V(x,y)$ gives rise to a Fraunhofer diffraction in the plane Γ. At the spatial coordinates (X,Y) in the lens focal plane Γ, the diffraction field $U(X,Y)$ is given by the Fraunhofer formula

$$U(X,Y)=\iint_D V(x,y)\exp\left[-i\frac{2\pi}{\lambda}\left(\frac{X}{f}x+\frac{Y}{f}y\right)\right]dxdy \qquad (3)$$

where f is the distance of the focal plane Γ from the lens, and the integration is taken over the area D of the object plane Π covered by the illuminated area on the surface. When standardizing the coordinates (X,Y) by the lens focal length f and the wavelength λ, $U(p,q)=U(X/\lambda f,\ Y/\lambda f)$ yields the Fourier transform of the object wave $V(x,y)$. Hence, we can obtain a mapping of the power spectrum of the object wave by measuring diffraction intensity $I(X,Y)=|U(X,Y)|^2$ then conversing the spatial coordinates (X,Y) into the spatial frequency coordinates (p,q). The information of the surface profile appears as the spectral intensity at the corresponding spatial frequency in the spatial frequency domain.

Although an object wave can be fully characterized by obtaining its Fourier spectrum completely, which is in general complex-valued function, the measured diffraction intensity gives access only to the second order information of the spectrum, i.e., power spectrum density. Thus, an inverse problem has to be solved to determine the phase from the knowledge of the power spectrum.

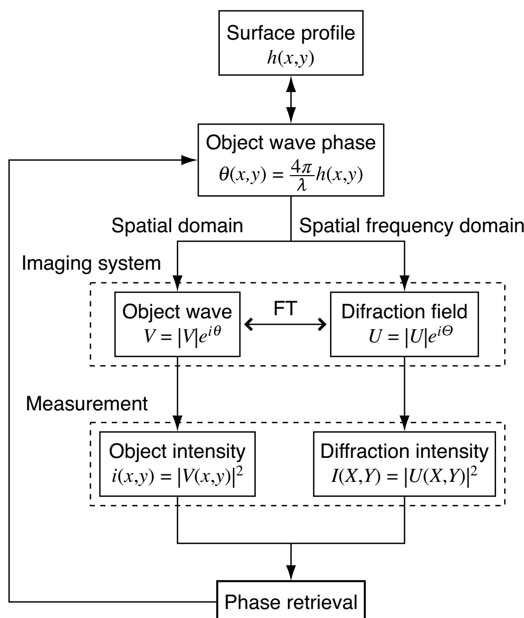

Fig. 2. Schema of surface reconstruction using phase retrieval technique.

Fig. 2 explains a schema of reconstructing the surface profile using phase retrieval technique. As described earlier, we obtain the power spectrum of the object wave by measuring diffraction intensity. In order to obtain sufficient information to determine the phase of the object wave, we measure the intensity of the object wave (object intensity) $i(x,y)=|V(x,y)|^2$ besides the diffraction intensity. From the pair of intensities measured both in the spatial and spatial frequency domains, phase retrieval can determine the phase of the object wave. Finally, surface profile is calculated from the determined phase.

2.2. Phase retrieval algorithm

A block diagram of the phase retrieval algorithm[4,5] is shown in Fig. 3. The algorithm involves iterative Fourier transform back and forth between the spatial and spatial frequency domain and application of the measured intensity data in each domain. Denoting an estimate of the phase for kth iteration, $\theta_k(x,y)$, the estimate of the object wave $g_k(x,y)$ is expressed as $g_k(x,y)=|V(x,y)|\exp[i\theta_k(x,y)]$. The following four steps are applied iteratively to this estimate $g_k(x,y)$: (1) Fourier transform an estimate of the object wave; (2) replace the modulus of the resulting computed Fourier transform with the measured Fourier modulus to form an estimate of the Fourier spectrum; (3) inverse Fourier transform the estimate of the Fourier spectrum; and (4) replace the modulus of the resulting computed function with the measured modulus to form a new estimate of the object wave. In equations this is,

$$G_k(p,q)=|G_k(p,q)|\exp[i\Theta_k(p,q)]=\Im[g_k(x,y)]\ , \qquad (4)$$

$$G'_k(p,q)=|U(p,q)|\exp[i\Theta_k(p,q)]\ , \qquad (5)$$

$$g'_k(x,y)=|g'_k(x,y)|\exp[i\theta'_k(x,y)]=\Im^{-1}[G'_k(p,q)]\ , \qquad (6)$$

$$g_{k+1}(x,y)=|V(x,y)|\exp[i\theta_{k+1}(x,y)]$$

$$=|V(x,y)|\exp[i\theta'_k(x,y)]\ , \qquad (7)$$

where $G_k(p,q)$ and $\Theta_k(p,q)$ are the estimate of the Fourier spectrum and its phase, and $\Im$ and $\Im^{-1}$ are Fourier transform operator and its inverse, respectively.

The convergence of the algorithm is monitored by calculating normalized rms error, E^2_k, defined in the spatial frequency domain by

$$E_k^2=\frac{\iint[|U(p,q)|-|G_k(p,q)|]^2dpdq}{\iint|U(p,q)|^2dpdq}\ . \qquad (8)$$

The value of rms error E^2_k decreases at each iteration[4]. The iterations continue until the value of error E^2_k converges to be sufficiently equal to zero or stays the same level

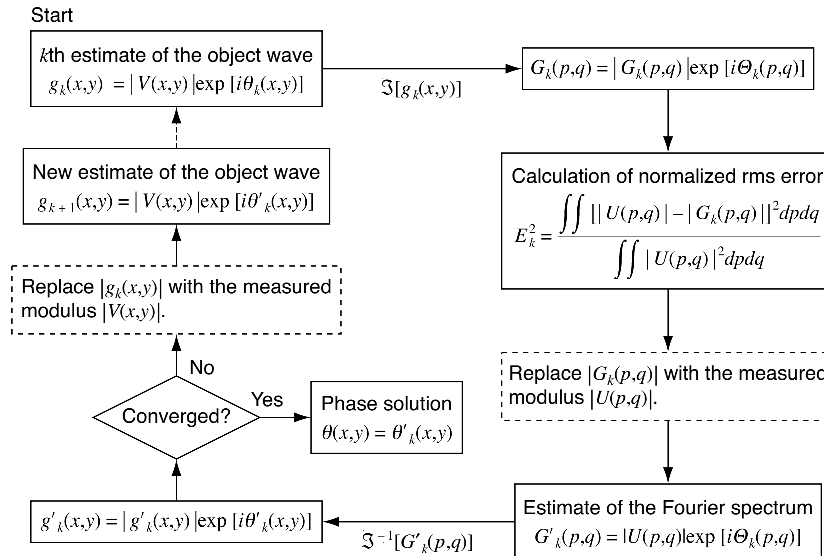

Fig.3 Block diagram of the phase retrieval algorithm.

with a number of further iterations. When the error E^2_k reaches a minimum, a solution has been found.

The solution of the algorithm is known to be almost always unique except for the minor ambiguities such as rotations by $2/\pi$, linear shifts, and multiplication by a unit magnitude complex constant[3]. In order to remove these minor ambiguities and further, lessen the computation time required, it is desirable to give an educated guess at the correct phase distribution as an initial estimate of the algorithm. Indeed, we are concerned here with engineering surfaces, which are usually processed according to the designed geometrical quantities such as dimensions or size parameters. These *a priori* known knowledge about engineering surface are to be used as the initial estimate of the iterative algorithm.

3. OPTICAL INSTRUMENTATION

We have developed an instrument on the basis of the general principles described in the previous section. The optical configuration of the developed instrument is shown in Fig. 4. An Ar ion laser (MELLES GRIOT 543-100BS; wavelength, 488nm) was used as a light source, and the laser light is introduced to the instrument by a singlemode optical fiber. A collimator lens and objective2 produce a laser spot of approximately 16μm in its diameter on the back focal point of the objective1. By this setup (Köhler's central illumination), specimen is illuminated by a normally incident Gaussian beam with its waist coincide with the specimen surface. There is no requirement of precise positioning of the specimen as a result of the large depth of focus.

Scattering light from the specimen surface is gathered by objective1 (Nikon CFIC-EPI PLAN ELWD, 50×, N.A. of 0.55, W.D. of 8.70mm), forming the Fraunhofer diffraction in its back focal plane; by exchanging objective1, different settings of resolution, field of view and working distance can be adjusted so as to suite an individual specimen. Note that the lateral resolution in the present method depends on the maximum spatial frequency that can be obtained by objective1, given by N.A./λ. We take a period $\Delta=\lambda$/N.A. as the theoretical criterion of the lateral resolution, the finest sinusoidal phase distribution resolvable in the spatial frequency domain. The diffraction image is magnified four-holds by a microscopy optical system consisting of objective2 (Nikon CFI PLAN, 4×, N.A. of 0.10, W.D. of 30mm) and a tube lens as indicated by path1 in Fig. 4. On the other hand, an optical microscope (path2 in the figure) focuses into a magnified image of the specimen surface on its image plane, which enables one to measure object intensity. A cooled CCD camera (Apogee Instruments AP4; Kodak KAF-4200; pixels, 2048×2048 of 9μm×9μm; dynamic range of > 75dB) is mounted on the instrument to measure intensity images. Two intensities are respectively

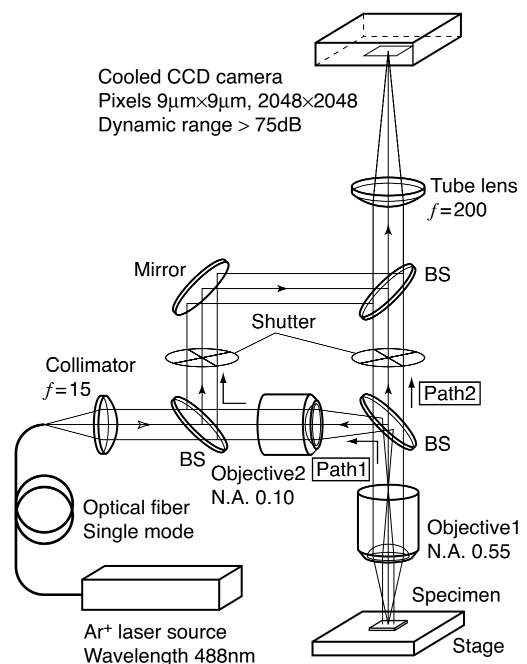

Fig. 4. Schematic illustration of the optical configuration. BS, beam splitter.

measured by opening and shutting two shutters to switch the paths. Measured images are passed to an image processor to remove undesirable artifacts and measurement noise. The instrument was placed in a cleanroom of class 5000. Photographs of the developed instrument are shown in Fig. 5. Two stages indicated in Fig. 5(a) are used for the alignments of the specimen and the illumination optics.

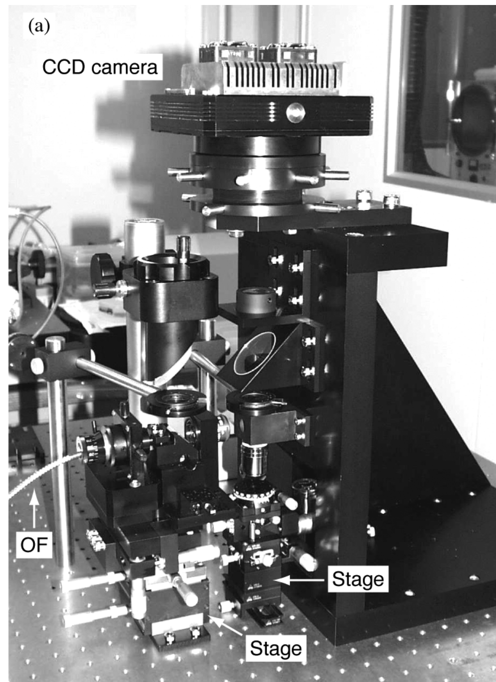

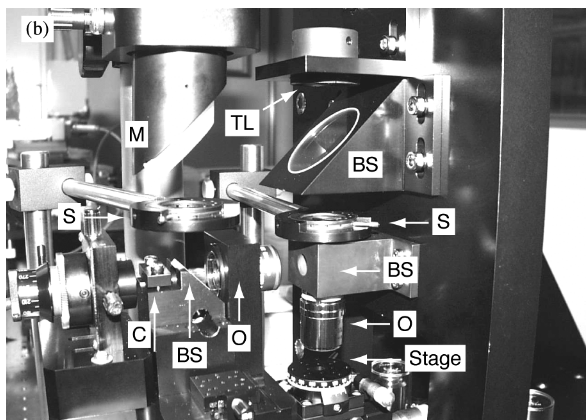

Fig. 5. Photograph of the developed instrument. (a) Overview. OF, optical fiber. (b) Detail: C, collimator; BS, beamsplitter; O, objective; S, shutter; M, mirror, TL, tube lens.

4. EXPERIMENTS

4.1. Measurement of diffraction and object intensities

The instrument was verified by measuring a surface topography reference that was designed for characterizing SPM. A sketch of the specimen (VLSI standards STR10-440P) is illustrated in Fig. 6(a). The specimen consists of an array of alternating bars and spaces with an uniform pitch of 10μm. The entire top surface of the die is coated with a uniform layer of platinum, and the depth of pockets are defined at 44nm. A sectional profile of the specimen obtained by AFM (Digital Instruments) is also shown in Fig. 6(b).

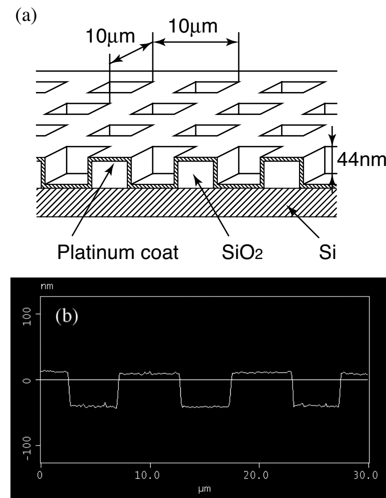

Fig. 6. (a) Sketch of the specimen. (b) Section profile of the specimen obtained by AFM.

A center of the specimen was illuminated. Measured diameter of the incident Gaussian beam was approximately 160μm at its waist. Throughout the intensity measurements, bias, dark, and sensitivity variations between each pixel in the CCD chip were calibrated to improve the signal-to-noise ratio of the represented intensity values in the CCD images. The lateral magnifications of the imaging system were also calibrated.

First, we measured the object intensity $i(x,y)=|V(x,y)|^2$. Obtained CCD image is shown in Fig. 7 – only the central part of the obtained image was cropped and shown here. Next, we measured the diffraction intensity. In order to obtain sufficient signals for the high-frequency components having weak intensities, we took two exposures with the exposure time controlled, then two images were properly combined. The obtained image of the diffraction intensity $I(X,Y)=|U(X,Y)|^2$ is shown in Fig. 8. Because the image contains intensity values distributed over wide dynamic range, gray levels of the presented image have been stretched into the logarithmic scale. A uniform separation of

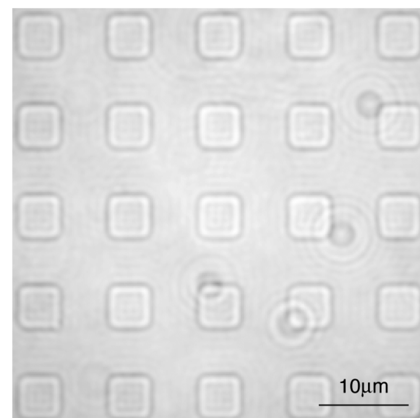

Fig. 7. Measured object intensity $i(x,y)=|V(x,y)|^2$. Only the central part of the obtained image was cropped and shown.

each component of the Fraunhofer pattern was observed, and high-order components having weak intensity can be distinguished clearly.

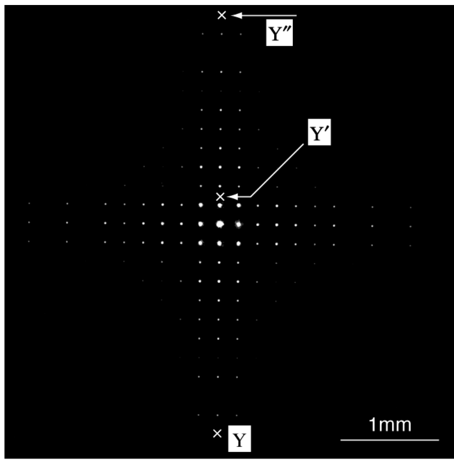

Fig. 8. Measured diffraction intensity $I(X,Y)=|U(X,Y)|^2$. Gray levels of the images are logarithmic. The scale bars correspond to a measure taken on the back focal plane of the objective1 (see Fig. 4).

We calculated power spectrum of the object wave from the measured diffraction intensity. The power spectrum along the line Y–Y″ in Fig. 8 is shown in Fig. 9(a). Fig. 9(b) is a detailed plot of the high-order spectral components

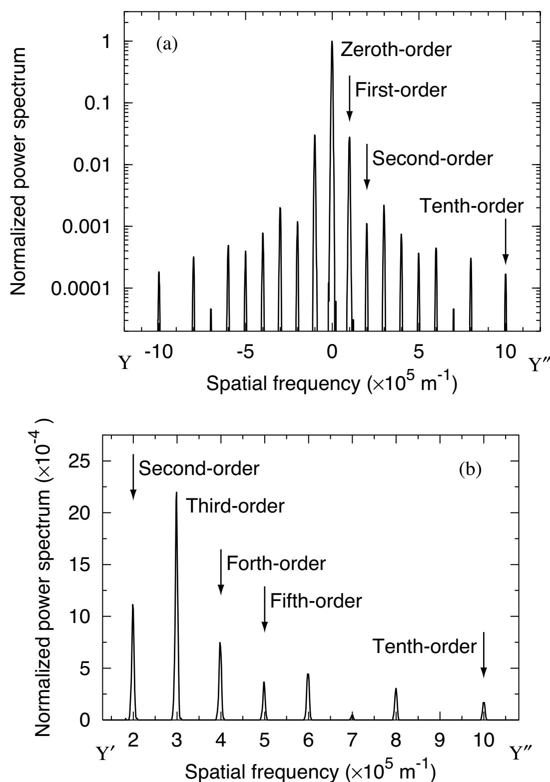

Fig. 9. Plot of power spectrum calculated from the measured diffraction intensity. The spectra are normalized by the principal maximum of the zeroth-order component. (a) Line plot along Y–Y″ in Fig. 8. (b) Detailed plot of the high-order spectra Y′–Y″ in Fig. 8.

corresponding to Y′–Y″ in Fig. 8. In these plots, spectra are normalized by the principal maximum of the zeroth-order component. The spectra up to tenth-order could be obtained, distributing over a dynamic range of more than 100dB. Each successive spectrum is uniformly separated by $10^5 m^{-1}$, i.e., the reciprocal of the nominal pitch of the specimen.

4.2. Surface reconstruction results and discussions

We performed the phase retrieval using the measured intensity data. An ideal surface profile according to the nominal dimensions of the specimens was used as the initial phase estimate of the algorithm, then 300 iterations were followed. A curve of normalized rms error E^2_k against the number of iteration is shown in Fig. 10. After the rapid decrease at the initial few iterations, the value of the normalized rms error decreased to approximately 0.04.

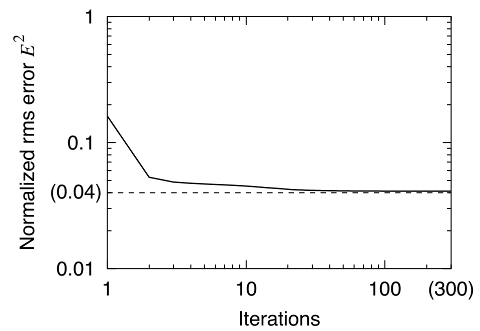

Fig. 10. Iterations vs normalized rms error.

The surface profile was calculated from the reconstructed phase by using (2), shown in Fig. 11. Each rectangular pocket having the width of 5μm is clearly distinguished. The diameter of the dashed circle in Fig. 11 corresponds to the beam diameter of the incident Gaussian beam, 160µm. Shapes of each pocket were uniformly reconstructed inside the circle, while outside of the circle, the reconstructed profile was distorted. This result indicates that the measurement area of the present method is almost the same as the beam diameter of the incident Gaussian beam.

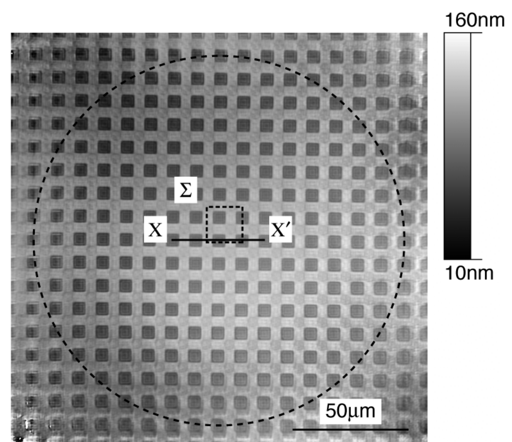

Fig. 11. Surface reconstructed by phase retrieval. Surface height is represented by gray level. Diameter of the dashed circle corresponds to the beam diameter of the illumination, 160µm.

The surface of area Σ and the section profile along line X–X′ in Fig. 11 are shown in Figs. 12(a) and 12(b), respectively. The dimensions of the measured profile are in good agreement with the nominal values of the specimen, pitch of 10µm and depth of 44nm. Further, we experimentally verified the lateral resolution by calculating the slope at the sidewall of the pockets in the measured profile. As indicated in Fig. 12(b), the value of the lateral resolution determined from the experimental data was well reproduced by the theoretically predicted value, λ/N.A.=0.89µm.

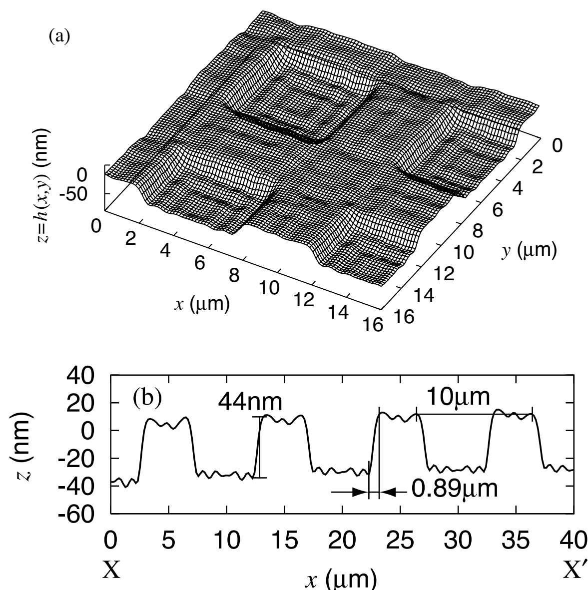

Fig. 12. (a) Surface plot of area Σ in Fig. 11. (b) Section profile along line X–X′ in Fig. 11.

One can observe that the measured profile is slightly waving, resulting in at most ±5nm measurement error in its height when compared with the one obtained by AFM (see also Fig. 6(b)). This measurement error is attributed to a physical property inherent in the coherent imaging. In the coherent imaging, the measured spectra are sharply dropped to zero outside the bandwidth of the system. This results in arising Gibbs phenomenon in the reconstructed profile (this is also referred to as ringing effect). Errors in the intensity measurements can also be counted as the other sources of this deviation in the reconstructed profile. Systematic error such as the imperfections of the CCD chip and the lens aberrations of the imaging system can be compensated to improve the accuracy of the reconstructed profile; the CCD-oriented problems can be removed by performing more careful calibrations of the CCD chip, while the error caused by the lens aberrations can be deconvolved on the basis of the OTF (Optical Transfer Function) of the present imaging system.

5. CONCLUSIONS

We have designed and developed an instrument based on the general principles of the optical inverse scattering phase method. In the present method, power spectrum of the micro-surface profile is obtained by measuring its Fraunhofer diffraction intensity. With the additionally measured object intensity, phase retrieval technique allows one to reconstruct deterministic surface profile from the power spectrum.

The developed instrument was verified by measuring a surface topography reference that was designed for characterizing SPM. The specimen consists of a grid pattern having rectangular pockets 44nm deep at intervals of 10µm. It was demonstrated that a surface profile is successfully reconstructed within the area inside the $1/e$ full width of a incident Gaussian beam. The dimensions of the measured surface were well consistent with the nominal values of the specimen. Further, good agreement between the surface profile measured by the present method and AFM was also obtained within the deviation of at most ±5nm in its height. These experimental results support the validity of the instrumentation as well as the proposed measurement principles.

The present method is suitable in applications to in-process or near-process as well as on-machine measurements of micro-surface profile in a production environment. Application to the measurement of non-periodic surface will be done in future work.

ACKNOWLEDGEMENTS

This study is partly supported by the JSPS Research Fellowships for Young Scientists (#01145).

REFERENCES

[1] T. Miyoshi, Y. Takaya, K. Saito, "Micromachined profile measurement by means of Optical Inverse Scattering Phase Method", *Ann. CIRP*, vol. 45, no. 1, pp. 497-500, 1996.

[2] A. Taguchi, T. Miyoshi, Y. Takaya, K. Saito, "3-D micro-profile measurement using Optical Inverse Scattering Phase Method", *Ann. CIRP*, vol. 49, no. 1, pp. 423-426, 2000.

[3] D.R. Luke, J.V. Burke, R.G. Lyon, "Optical wavefront reconstruction: theory and numerical method", *SIAM Review*, vol. 44, no. 2, pp. 169-224, 2002.

[4] R.W. Gerchberg, W.O. Saxton, "A practical algorithm for the determination of phase from image and diffraction plane pictures", *Optik*, vol. 35, no. 2, pp. 237-246, 1972.

[5] J.R. Fienup, "Phase retrieval algorithms: a comparison", *Appl. Opt.*, vol. 21, no. 15, pp. 2758-2769, 1982.

Authors: Atsushi Taguchi; Department of Mechanical Engineering and Systems, Osaka University, Suita, Osaka 565-0871, Japan; phone: +81-6-6879-7321; fax: +81-6-6879-7320; e-mail: taguchi@optim.mech.eng.osaka-u.ac.jp;
Takashi Miyoshi; Department of Mechanical Engineering and Systems, Osaka University, Suita, Osaka 565-0871, Japan; phone: +81-6-6879-7319; fax: +81-6-6879-7320; e-mail: miyoshi@mech.eng.osaka-u.ac.jp;
Yasuhiro Takaya; Department of Mechanical Engineering and Systems, Osaka University, Suita, Osaka 565-0871, Japan; phone: +81-6-6879-7320; fax: +81-6-6879-7320; e-mail: takaya@mech.eng.osaka-u.ac.jp;
Satoru Takahashi; Department of Precision Engineering, University of Tokyo, Hongo, Bunkyo-ku, Tokyo 113-8656, Japan; phone: +81-3-5841-6451; e-mail: takahashi@nano.pe.u-tokyo.ac.jp